Molecular Therapy
Nucleic Acids
Original Article

miR-17-5p Regulates Heterotopic Ossification by Targeting ANKH in Ankylosing Spondylitis

Xiong Qin,[1,2,3,5] Bo Zhu,[2,3,5] Tongmeng Jiang,[2,3,4,5] Jiachang Tan,[1] Zhenjie Wu,[1] Zhenchao Yuan,[1] Li Zheng,[2,3] and Jinmin Zhao[2,3,4]

[1]Department of Bone and Soft Tissue, Affiliated Tumor Hospital of Guangxi Medical University, 530021 Nanning, China; [2]Guangxi Engineering Center in Biomedical Materials for Tissue and Organ Regeneration, Guangxi Medical University, 530021 Nanning, China; [3]Guangxi Collaborative Innovation Center for Biomedicine, Guangxi Medical University, 530021 Nanning, China; [4]Guangxi Key Laboratory of Regenerative Medicine & International Joint Laboratory on Regeneration of Bone and Soft Tissue, Guangxi Medical University, Nanning, 530021, China

Ankylosing spondylitis (AS) is a chronic inflammatory disease characterized with heterotopic ossification of the axis joints ligaments, resulting in joint disability. MicroRNAs (miRNAs) are regulators of mRNAs that play a crucial role in the AS pathological process. Here, we showed that the level of miR-17-5p was significantly higher in fibroblasts and ligament tissues from AS patients as compared to the non-AS individuals. Knockdown of the miR-17-5p from the fibroblasts derived from AS patients exhibited decreased osteogenic differentiation and ossification. On the other hand, AS patient-derived fibroblasts overexpressing miR-17-5p displayed the increased osteogenesis. Furthermore, inhibition of miR-17-5p ameliorated osteophyte formation, and the sacroiliitis phenotype in AS rats received emulsified collagen. Mechanistically, miR-17-5p regulated osteogenic differentiation by targeting the 3′ UTR of ankylosis protein homolog (*ANKH*). Also, downregulation of miR-17-5p slowed AS progression through regulation of cytokines, such as dickkopf-1 (DKK1) and vascular endothelial growth factor (VEGF). In conclusion, our findings reveal a role of the miR-17-5p-*ANKH* axis in the regulation of heterotopic ossification, which is essential for therapeutic intervention in heterotopic ossification in AS.

INTRODUCTION

Ankylosing spondylitis (AS) is a chronic inflammatory arthritis of the axial skeleton that is characterized by inflammatory back pain, stiffness, altered buttock pain, and joint gelling.[1] The hallmark of AS is neo-ligament ossification at the axis joints.[2] Pathological bone formation results in the sacroiliac joint and axial spine to undergo ankylose, eventually leading to loss of joint function and disability.[3] Currently, there is no effective method to prevent the ossification of the ligaments at the axis joints.

MicroRNAs (miRNAs), a class of endogenous, non-coding, RNA-modulating mRNAs, have been reported to regulate AS progression by interacting with genes that are potential biomarkers for AS.[4,5] Serum levels of miR-146a, miR-29a, and miR-155 were significantly upregulated in patients with AS.[6,7] Among these miRNAs, miR-10b-5p was a novel T helper (Th)17 regulator in Th17 cells derived from AS patients.[8] A large-scale microarray analysis in AS patients showed 22 highly enriched miRNAs, including miR-17-5p and miR-27b-3p, which were associated with the osteogenic differentiation potentials of ligament-derived fibroblasts.[9] Our pilot study, based on miRNA expression profiling, showed differentially expressed miR-17-5p in AS patients compared with that in non-AS controls. miR-17-5p was reported as a significant regulator in the pathological process of reactive astrogliosis after spinal cord injury by affecting cell-cycle machinery.[10] However, the role of miR-17-5p in the regulation of AS remains unknown.

Cellular pyrophosphate exportation contributes to the pathological ossification during AS progression,[11] which is regulated by pyrophosphate transfer-related genes,[12,13] such as *ANKH*.[14] *ANKH*-deficient mice have been reported to present symptoms similar to those of AS patients, including gradually narrowed joint space, ossified intervertebral discs and spine ligaments, and a stiff spine.[15] Recent studies have shown that *ANKH*-OR (polymorphism in the 5′-non-coding region) and *ANKH*-TR (polymorphism in the promoter region) are novel genetic markers that are closely associated with AS.[16] The variation in the *ANKH* gene is associated with increased susceptibility to AS in the Northern Han Chinese population. The relationship between the *ANKH* haplotype (rs26307/rs27356) and the risk of AS incidence suggests that the minor alleles rs26307(T)/rs27356(C) are protective factors for AS.[17] Our TargetScan and miRanda analyses showed the association of miR-17-5p with *ANKH*, indicating that miR-17-5p might regulate AS pathological ossification via *ANKH*.

Received 22 August 2019; accepted 1 October 2019;
https://doi.org/10.1016/j.omtn.2019.10.003.

[5]These authors contributed equally to this work.

Correspondence: Li Zheng, Guangxi Engineering Center in Biomedical Materials for Tissue and Organ Regeneration, Guangxi Medical University, 530021 Nanning, China.
E-mail: zhengli224@163.com
Correspondence: Jinmin Zhao, Guangxi Engineering Center in Biomedical Materials for Tissue and Organ Regeneration, Guangxi Medical University, 530021 Nanning, China.
E-mail: zhaojinmin@126.com

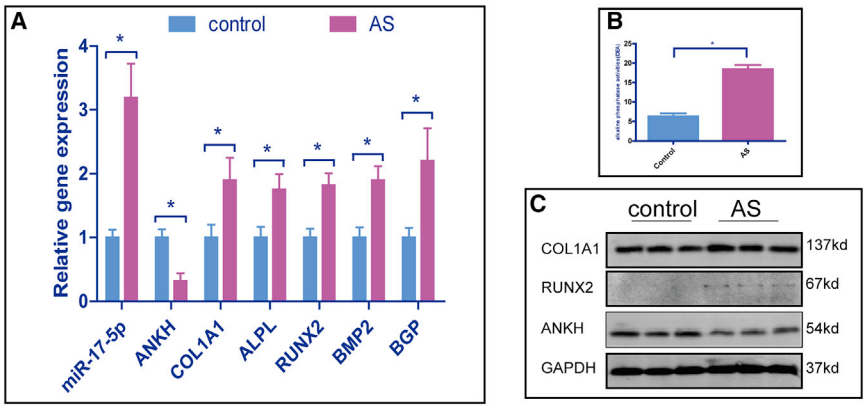

Figure 1. Differential Expression of miR-17-5p, ANKH, and Osteogenesis Differentiation Analysis in Human AS and Non-AS Ligament Tissues

(A) The quantitative real-time PCR analysis of miR-17-5p, ANKH, ALPL, COL1A1, BGP, BMP2, and RUNX2 mRNA levels in human AS or non-AS ligament tissues. The relative expression of miR-17-5p was normalized to U6, and the remaining relative mRNA expression levels were normalized to GAPDH by using a comparative Ct method. Error bars: mean ± SD (n = 3). *p < 0.05. (B) Determination of alkaline phosphatase activity of the ligament tissues. Error bars: mean ± SD (n = 3). *p < 0.05. (C) The protein expression of osteogenesis-related genes (COL1A1 and RUNX2) and ANKH was analyzed by western blot in ligament tissues. GAPDH was used as the loading control.

In this study, we used AS patient-derived fibroblasts for *in vitro* studies and emulsified collagen-induced AS rat models to investigate the role of miR-17-5p on AS ossification by miR-17-5p silencing and overexpression. This study may provide a novel therapeutic option for AS.

RESULTS

The Ligament Tissues from AS Patients Exhibit Increased miR-17-5p Expression and Reduced ANKH Expression with a Higher Osteogenesis

To determine whether miR-17-5p plays a role in the pathogenesis of AS in humans, we analyzed the ligament tissues from AS patients and those non-AS controls for the expressions of miR-17-5p by quantitative real-time PCR. The miR-17-5p expression in the ligament tissues from AS patients was higher than that of non-AS controls (Figure 1A). The comparison between human ligament tissues from AS samples and those from the non-AS controls revealed that high miR-17–5p expression in the ligament tissues of AS patients was accompanied by high expression of genes associated with osteoblast differentiation, including *BMP2*, *BGP*, *COL1A1*, *RUNX2*, and *ALPL* (Figure 1A), indicating osteogenic potential of the ligament tissues that potentially explained the ectopic ossifications of the ligament tissues in AS patients. The osteogenic phenotype of ligament tissues in AS was further confirmed by increased alkaline phosphatase (ALP) activity (Figure 1B). Higher levels of COL1A1 and RUNX2 in ligament tissues from AS patients were confirmed by western blot analysis. The protein levels of both COL1A1 and RUNX2 in the AS ligament tissues were higher than those in non-AS ligament tissues (Figure 1C). We also detected a lower level of the pyrophosphate transfer-related gene, *ANKH*, expressed in ligament tissues from AS than those from non-AS patients, measured by both quantitative real-time PCR and western blot (Figures 1A and 1C). Taken together, these data showed that the ligament tissues from AS patients expressed high levels of miR-17-5p and low levels of *ANKH* and had higher osteogenesis compared to the non-AS controls.

The Fibroblasts from AS Patients Express High Levels of miR-17-5p and Show an Apparent Osteogenic Differentiation

To detect whether the ligament tissue-derived fibroblasts from AS patients are sensitized to osteogenic differentiation, the fibroblasts from the ligament tissues of AS and non-AS patients were isolated and examined. H&E and immunocytochemistry staining were used to evaluate the characteristics of the fibroblasts. Similar cellular morphometry with long fusiform or flat star-shaped cells with ovoid nuclei were observed in the fibroblasts isolated from the ligament tissues of AS and non-AS patients stained by H&E. Of note, immunocytochemistry staining with vimentin antibody, a specific marker for fibroblasts, showed that the fibroblasts from the AS group expressed fewer vimentin (dark brown) than fibroblasts from the non-AS group (Figure 2A), indicating that the fibroblasts from AS patients had altered morphometry and osteogenic differentiation.

To assess the characterization of ossification of the fibroblasts from AS patients and investigate the relationship of miR-17-5p with ectopic osteogenesis in fibroblasts, the expression levels of miR-17-5p and osteogenic-related genes, as well as ALP activity, were examined in fibroblasts isolated from AS and non-AS patients. The quantitative real-time PCR analysis showed that the level of miR-17-5p mRNA in the fibroblasts from AS patients was higher than that in non-AS fibroblasts (Figure 2B). However, *ANKH* mRNA and protein expression levels were remarkably low in fibroblasts from AS patients compared with fibroblasts from non-AS patients (Figures 2B and 2C). As expected, the mRNA expression of osteogenic-related genes, including *BMP2*, *BGP*, *COL1A1*, *RUNX2*, and *ALPL*, was elevated in the AS patient-derived fibroblasts compared with those of the non-AS patient-derived fibroblasts (Figure 2B). Western blot analysis also showed that the protein expression levels of COL1Al and RUNX2 were consistently increased in fibroblasts from AS patients (Figure 2C). Moreover, the fibroblasts from ligament tissues of AS patients exhibited more intense ALP staining (5-bromo-4-chloro-3-indolyl phosphate/nitro blue tetrazolium [BCIP/NBT]) (Figure 2D) and higher ALP activity compared with non-AS patient-derived fibroblasts (Figure 2E). These results were consistent with those from the ligament tissue. Also, increased calcified nodules appeared in AS patient-derived fibroblasts, as observed by Alizarin red staining (ARS), indicating an increased mineralization level in fibroblasts from AS patients (Figure 2D). Taken together, these data suggested that the AS patient-derived

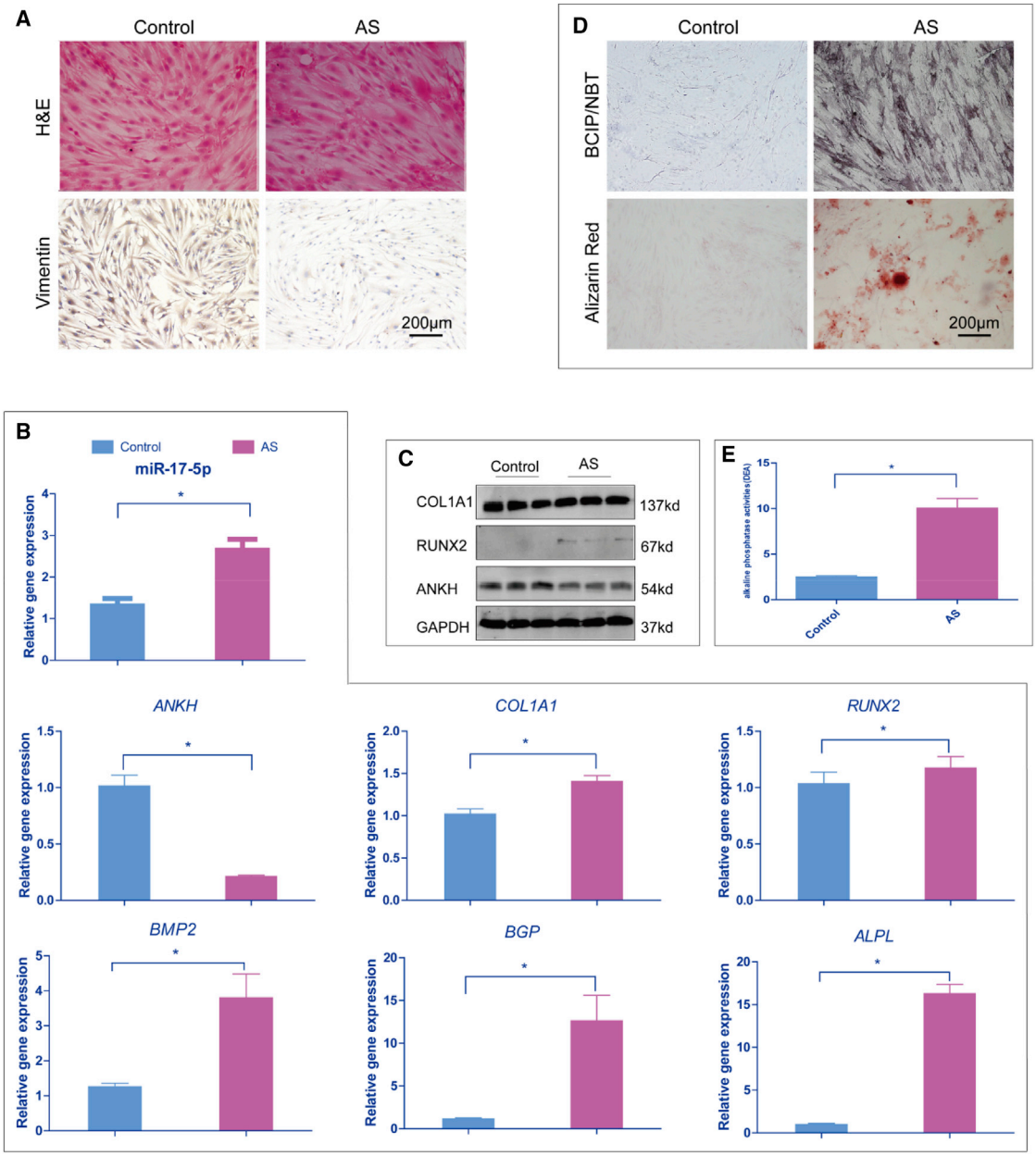

Figure 2. The Fibroblasts from AS Patient-Derived Ligament Tissues Show an Evident Osteogenic Differentiation Tendency

(A) Characterization of fibroblasts derived from non-AS and AS patient-derived fibroblasts was confirmed by using H&E staining (top) and immunohistochemistry staining with vimentin antibody (bottom). Scale bar: 200 μm. (B) The quantitative real-time PCR analysis of miR-17-5p, ANKH, ALPL, COL1A1, BGP, BMP2, and RUNX2 mRNA levels in non-AS fibroblasts and AS patient-derived fibroblasts. The relative expression of miR-17-5p was normalized to U6, and the remaining relative mRNA expression was normalized to GAPDH by using a comparative Ct method. Error bars: mean ± SD (n = 3). *$p < 0.05$. (C) The protein expression of osteogenesis-related genes (COL1A1 and RUNX2) and ANKH was analyzed by western blot in non-AS fibroblasts and AS patient-derived fibroblasts. GAPDH was used as the loading control. (D) BCIP/NBT staining (top) for ALP and Alizarin red staining (bottom) for mineralization in non-AS fibroblasts and AS patient-derived fibroblasts. Scale bar: 200 μm. (E) Determination of alkaline phosphatase activity in non-AS fibroblasts and AS patient-derived fibroblasts. Error bars: mean ± SD (n = 3). *$p < 0.05$.

fibroblasts expressed high levels of miR-17-5p, expressed low levels of *ANKH*, and showed an increased osteogenesis, indicating that miR-17-5p overexpression might potentiate the fibroblast cells to osteogenic differentiation.

miR-17-5p Represses ANKH by Targeting Its 3′ UTR

Given our observation that an inverse correlation between the expression of miR-17-5p and *ANKH* was found in both AS patient-derived fibroblasts and ligament tissues, we next sought to determine the

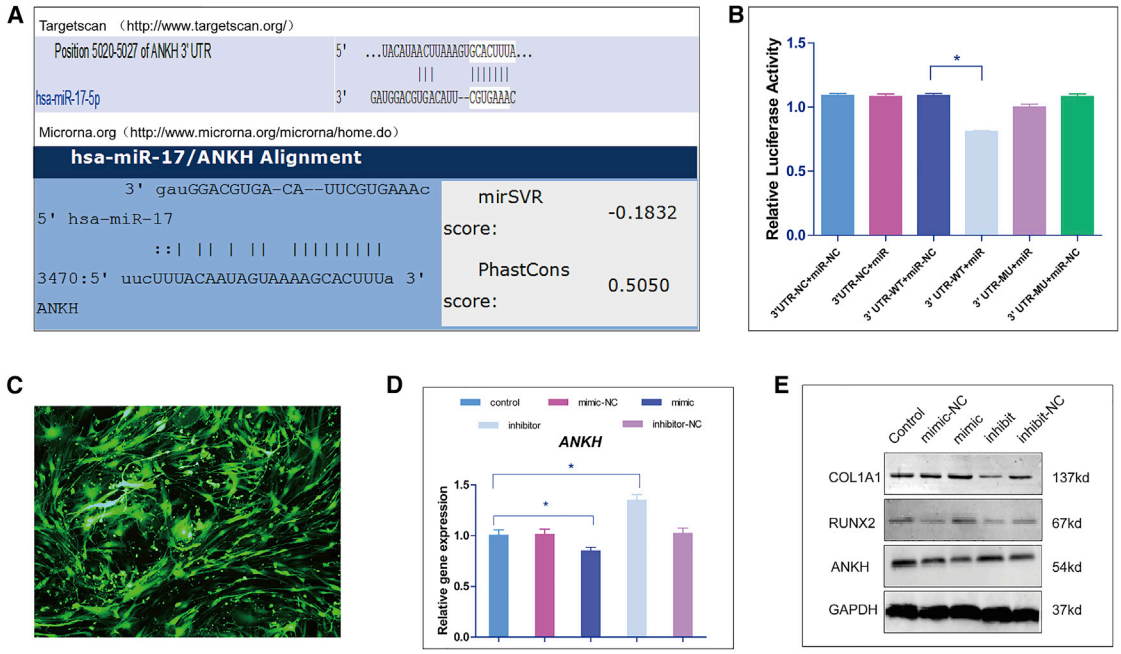

Figure 3. miR-17-5p Inhibits ANKH Expression through Its 3′ UTR

(A) The "seed" sequence of miR-17-5p was identified within the ANKH 3′ UTR by TargetScan and microRNA.org. (B) Luciferase activity was determined in HEK293T cells after co-transfection with miR-17-5p mimic/miR-NC and ANKH 3′ UTR-WT/MU reporter plasmids using a dual luciferase reporter system. Error bars: mean ± SD (n = 3). *p < 0.05. NC, negative control; WT, wild-type; MU, mutant; miR, miRNA-17-5p. (C) Transfection efficiency of fibroblasts was assessed by fluorescence microscopy after 72 h of transfection with the indicated viral vector (green). (D) The quantitative real-time PCR analysis of ANKH mRNA levels in AS patient-derived fibroblasts after treatment with miR-17-5p mimics or miR-17a-5p inhibitor. These data were normalized to GAPDH by using a comparative Ct method. Error bars: mean ± SD (n = 3). *p < 0.05. NC, negative control. (E) The protein expression of osteogenesis-related genes (COL1A1 and RUNX2) and ANKH was analyzed by western blot in fibroblasts after treatment with miR-17-5p mimics or miR-17-5p inhibitor. GAPDH was used as the loading control. NC, negative control.

interaction between miR-17-5p and *ANKH*. Our results from the miRNA target prediction databases TargetScan and microRNA.org suggested that *ANKH* was one of predicted target genes for miR-17-5p and was known to be involved in the pathogenesis of AS. A highly conserved sequence complementary to the "seed" sequence of miR-17-5p was identified within the *ANKH* 3′ UTR (Figure 3A). To test whether miR-17-5p directly targeted *ANKH*, we identified a putative recognition site in the *ANKH* 3′ UTR by utilizing TargetScan and constructed luciferase reporters that had either a wild-type 3′ UTR (*ANKH*-3′ UTR-WT) or an *ANKH* 3′ UTR containing mutant sequences of the miR-17-5p binding site (*ANKH*-3′ UTR-MU). In HEK293T cells, the luciferase activity of the wild-type *ANKH* 3′ UTR was significantly repressed by miR-17-5p, and mutation of the miR-17-5p binding site in the *ANKH* 3′ UTR reduced the repression (Figure 3B), indicating that the miR-17-5p binding site to the *ANKH* 3′ UTR was primarily responsible for the binding of miR-17-5p and the inhibition of *ANKH*. High transfection efficiency of fibroblasts was confirmed by fluorescence microscopy after 72 hours of transfection with the indicated viral vector (Figure 3C). To define further the role of miR-17-5p on *ANKH* in AS pathogenesis, overexpression and knockdown experiments were conducted using specific miR-17-5p mimics and a miR-17-5p inhibitor in fibroblasts derived from the ligament tissue of AS patients *in vitro*. We found that the mRNA level of *ANKH* was markedly decreased or elevated, respectively, following the administration of the miR-17-5p mimics or miR-17-5p inhibitor in the fibroblasts from AS patients compared with the cells transfected with an empty vector (Figure 3D). Moreover, the amount of ANKH protein was upregulated by transfection with the miR-17-5p inhibitor and remained low following treatment with miR-17-5p mimics (Figure 3E). These findings further suggested that miR-17-5p inhibited the expression of *ANKH* by targeting its 3′ UTR.

miR-17-5p Promotes Osteogenic Differentiation in Fibroblasts from Patients with AS

To investigate whether the increased abundance of miR-17-5p governs osteogenic differentiation of fibroblasts derived from the ligament tissue of AS patients, we next altered the miR-17-5p level in cells by treating fibroblasts with miR-17-5p mimics or the miR-17-5p inhibitor and measured the expression level of osteogenic transcripts and ALP activity. As expected, compared with transfection of the negative control (NC), the relative mRNA expressions of the osteogenic genes *BMP2*, *ALPL*, *RUNX2*, *COL1Al*, and *BGP* were significantly increased by transfection of miR-17-5p mimics (Figure 4A), as well as the expression levels of RUNX2 and COL1A1 proteins (Figure 3E). In contrast, the mRNA expressions of these osteogenic markers were reduced by transfection of the miR-17-5p inhibitor (Figure 4A), including RUNX2 and COL1A1 protein levels (Figure 3E). Functionally, ALP activity was substantially higher in the

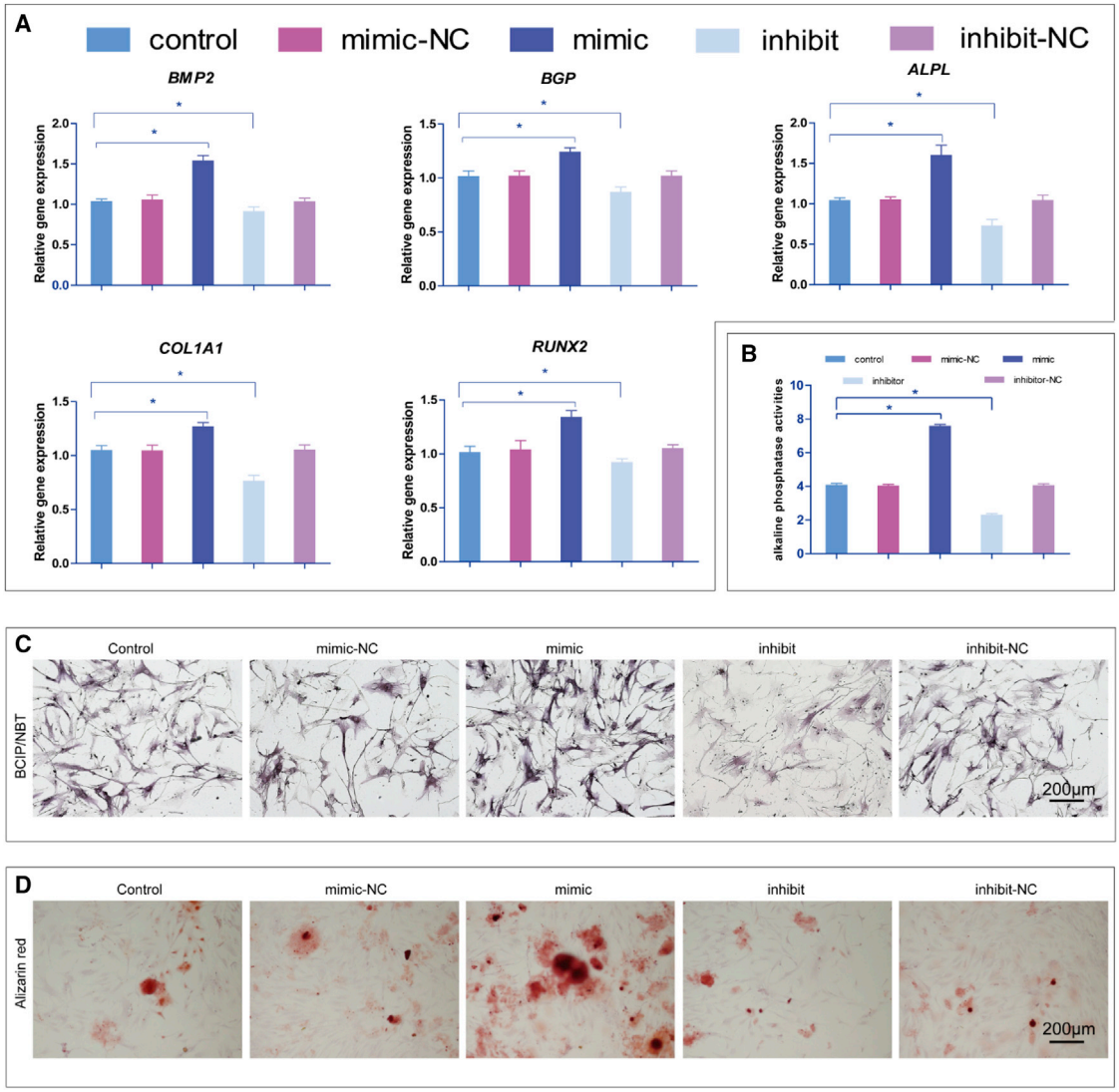

Figure 4. miR-17-5p Promotes Osteogenic Differentiation in Fibroblasts from Patients with AS

(A) The quantitative real-time PCR analysis of ALPL, COL1A1, BGP, BMP2, and RUNX2 mRNA levels in AS patient-derived fibroblasts after treatment with miR-17-5p mimics or miR-17a-5p inhibitor. These data were normalized to GAPDH by using a comparative Ct method. Error bars: mean ± SD (n = 3). *p < 0.05. NC, negative control. (B) Detection of alkaline phosphatase activity of AS patient-derived fibroblasts after infection with miR-17-5p mimics, miR-17-5p inhibitor, or negative control plasmid. Error bars: mean ± SD (n = 3). *p < 0.05. NC, negative control. (C) BCIP/NBT staining for ALP in fibroblasts after treatment with miR-17-5p mimics or miR-17a-5p inhibitor. NC, negative control. Scale bar: 200 μm. (D) Alizarin red staining for mineralization in fibroblasts after treatment with miR-17-5p mimics or miR-17a-5p inhibitor. NC, negative control. Scale bar: 200 μm.

miR-17-5p-mimic treatment group and markedly lower in the miR-17-5p-inhibitor treatment group as compared to their corresponding control treatment groups (Figure 4B). Consistent with the changes in ALP activity, we found that miR-17-5p mimics had enhanced ALP staining, whereas the miR-17-5p inhibitor had reduced ALP staining in AS patient-derived fibroblasts (Figure 4C). Additionally, the mineralization level visualized by ARS showed more mineral deposition in miR-17-5p-mimic-treated cells and less mineral deposition in miR-17-5p-inhibitor-treated cells compared with each corresponding control, mimic-NC- and inhibit-NC-treated group (Figure 4D). These results revealed that miR-17-5p positively regulates osteogenic differentiation of fibroblasts derived from AS patients.

A human cytokine antibody array was used to examine the cytokine levels in the miR-17-5p mimics- and inhibitor-conditioned medium. Subtractive analysis revealed that the secreted cytokine dickkopf-1 (DKK1) was decreased, and the vascular endothelial growth factor (VEGF) was increased in the miR-17-5p mimic-conditioned medium; however, increased VEGF and reduced DKK1 abundance was significantly reversed in the miR-17-5p inhibitor-conditioned medium

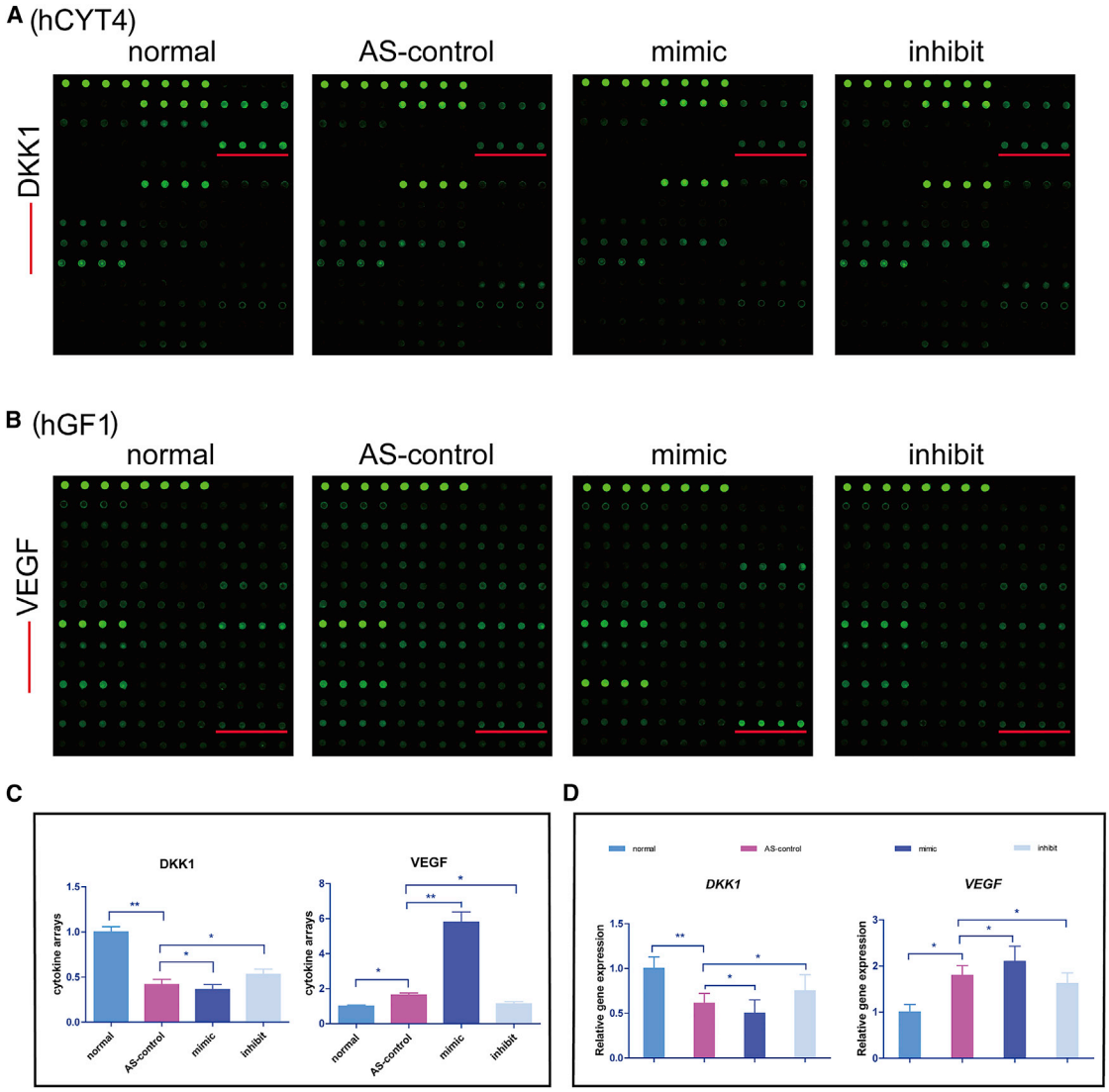

Figure 5. miR-17-5p Inhibits DKK1 and Elevates VEGF Levels in AS Patient-Derived Fibroblasts

Human cytokine antibody array analysis of the conditioned medium from either control or miR-17-5p-mimic/inhibitor-transduced fibroblasts indicated an altered abundance of DKK1 (A) and VEGF (B). Red underlining indicates DKK1 and VEGF. (C) The quantification of DKK1 and VEGF levels in response to (A) and (B), respectively. Error bars: mean ± SD (n = 3). *p < 0.05, **p < 0.01. (D) The quantitative real-time PCR analysis of DKK1 and VEGF mRNA levels in the conditioned medium from control or miR-17-5p-mimic/inhibitor-transduced fibroblasts. These data were normalized to GAPDH by using a comparative Ct method. Error bars: mean ± SD (n = 3). *p < 0.05, **p < 0.01.

(Figures 5A–5C). mRNA expression by quantitative real-time PCR confirmed that DKK1 mRNA was reduced, and VEGF mRNA was increased in the medium with fibroblasts overexpressing miR-17-5p, whereas in the miR-17-5p inhibitor-conditioned medium, DKK1 and VEGF mRNA levels showed the opposite trends (Figure 5D).

miR-17-5p Targeting Hinders the Progress of Sacroiliitis in the AS Rat Model

We investigated the role of miR-17-5p *in vivo* using an AS rat model. After 7 days of emulsified collagen sensitization in the four limbs of the animals, particularly the hind limbs exhibited swelling and redness. After 14 days, the rats showed swelling, congestion, restricted joint activity, and a stiff spine. An increased arthritis index[18] indicated the successful establishment of the AS rat model. The rats without collagen sensitization, which were used as a control, did not display any detectable defects in spinal morphology or histology. Compared to non-AS rats, AS rat models showed higher miR-17-5p expression in the ligament tissues (Figure 6A). Furthermore, the mRNA level of the miR-17-5p target gene, *Ankh*, was much lower in AS rats than in non-AS rats. Additionally, we found that the mRNA expressions of the osteogenic-related genes *Bmp2*, *Alpl*, *Runx2*, *Col1al*, and *Bgp*

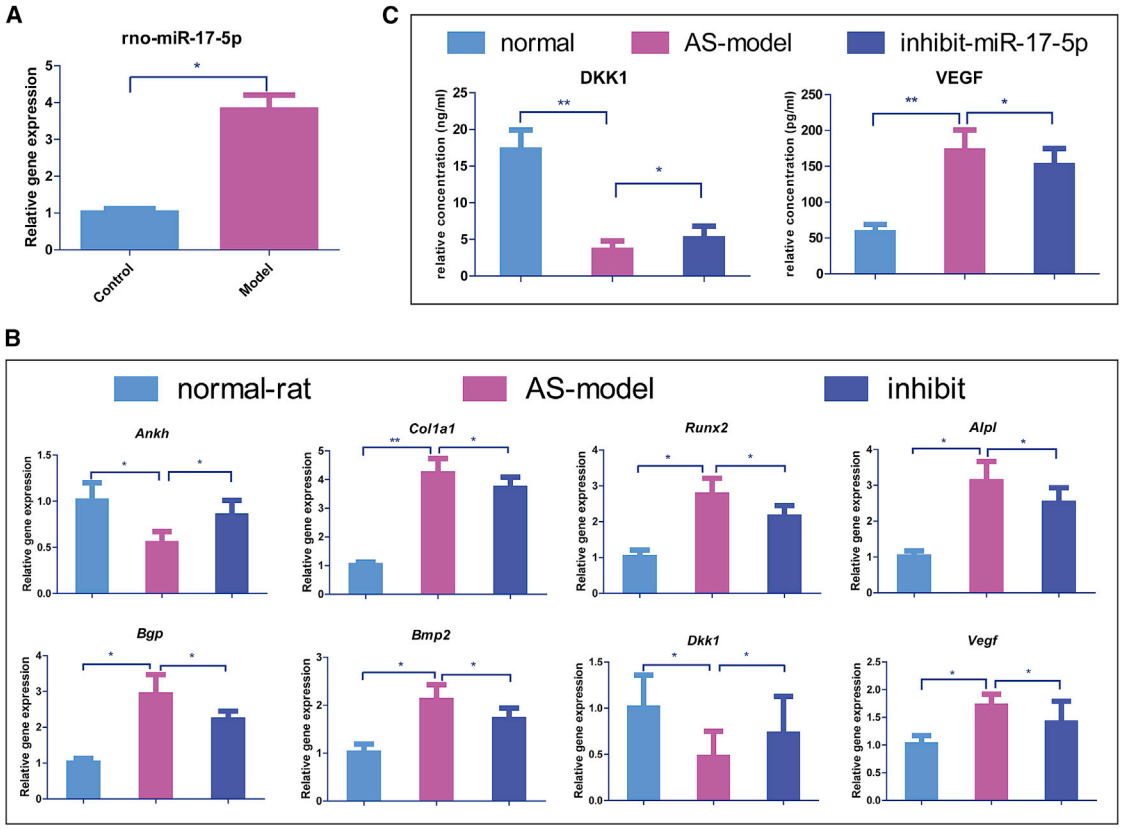

Figure 6. The Impact of miR-17-5p Absence on Osteogenesis-Related Gene Expression in an AS Rat Model

(A) The quantitative real-time PCR analysis of miR-17-5p mRNA levels in ligament tissues from the animal model. The relative expression of miR-17-5p was normalized to U6 by using a comparative Ct method. Error bars: mean ± SD (n = 3). *p < 0.05. (B) The quantitative real-time PCR analysis of Ankh, Alpl, Col1al, Bgp, Bmp2, Runx2, Dkk1, and Vegf mRNA levels in ligament tissues from AS rat models after treatment with lentivirus carrying shRNA for miR-17-5p or nontreatment. These data were normalized to GAPDH by using a comparative Ct method. Error bars: mean ± SD (n = 3). *p < 0.05, **p < 0.01. (C) The quantitative analyses of ELISA for DKK1 and VEGF production confirmed that their altered abundance in AS rat models was treated with lentivirus carrying shRNA for miR-17-5p. Error bars: mean ± SD (n = 3). *p < 0.05, **p < 0.01.

were markedly higher in the AS rat group compared to the non-AS rat group (Figure 6B). These findings were consistent with the results we had from human specimens.

To test if inhibition of miR-17-5p could rescue the sacroiliitis phenotype of AS rats, lentivirus carrying small hairpin RNA (shRNA) for miR-17-5p was injected into the AS rat when joints of the rat began to appear red and swollen at day 7. First, we examined the role of miR-17-5p in ectopic osteogenesis of the ligament tissue *in vivo*. The quantitative real-time PCR analysis for the whole ligament tissue showed that miR-17-5p inhibition downregulated osteogenic-related genes *Bmp2*, *Alpl*, *Runx2*, *Col1al*, and *Bgp* mRNA levels and promoted *Ankh* expression (Figure 6B). Moreover, quantitative analyses by ELISA confirmed that cytokine DKK1 was reduced, and VEGF was increased in AS rats. The changes in DKK1 and VEGF levels were reversed by lentivirus-mediated miR-17-5p downregulation in AS rats; i.e., miR-17-5p inhibition significantly upregulated and downregulated the levels of DKK1 and VEGF, respectively (Figure 6C). These results were confirmed by quantitative real-time PCR analysis (Figure 6B).

We used computed radiography and microscopic computed tomography (micro-CT) to detect osteophytes formation in the ligaments around the spine in AS rats. After 12 weeks of injection with lentivirus carrying shRNA for miR-17-5p, micro-CT revealed that the axial skeleton (sacroiliac joints and spine) showed marked osteophyte formation at the periphery of the spine in AS rats, which was alleviated by treatment with the miR-17-5p inhibitor (Figure 7A). We observed a noticeable increase in radiographic grading of sacroiliitis in the AS rats compared with the WT rats via micro-CT analysis, which is an earlier radiographic manifestation of AS and is required for an AS diagnosis.[19] In addition, the AS rats exhibited medial radiopacity over 12 weeks, indicating a heterotopic ossification surrounding the spine. However, inhibition of miR-17-5p ameliorated the sacroiliitis phenotype in AS rats (Figure 7B).

H&E and Masson staining were carried out to evaluate further the pathological changes in the sacroiliac joint of AS rat models. As shown in Figure 7C, inflammation was apparent in the sacroiliac joint in AS rats, whereas lentivirus carrying shRNA for miR-17-5p retained visible space in the sacroiliac joint, accompanied by reduced

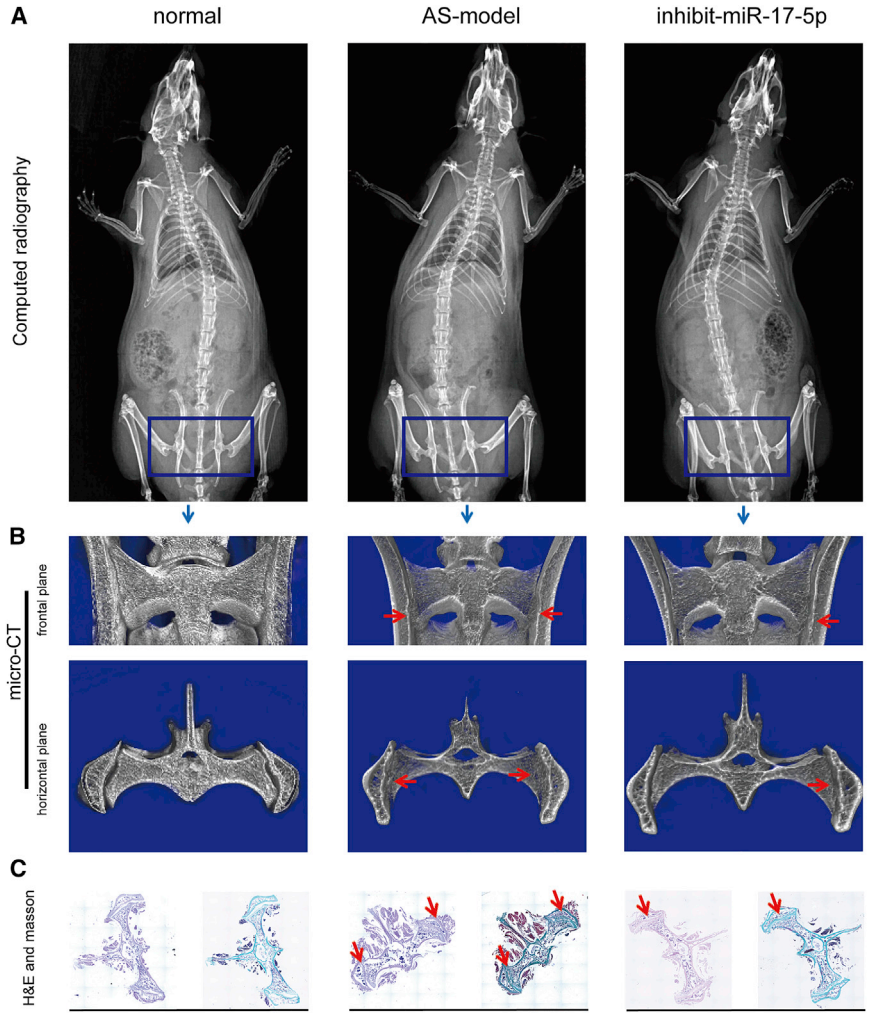

Figure 7. Therapeutic Inhibition of miR-17-5p Ameliorated the Sacroiliitis Phenotype in the AS Rat Model

(A) The skeletal structures of the animal model based on computed radiography. The box indicates sacroiliac joints. (B) The structure of the sacroiliac joint of the animal model according to micro-CT. (C) H&E and Masson staining for the sacroiliac joint of the animal model.

inflammation in these treated rats. Taken together, these findings demonstrated that inhibition of miR-17-5p slows the progression of sacroiliitis in AS rats.

DISCUSSION

In this study, we demonstrated that miR-17-5p has an essential role in directing fibroblasts into osteoblastic differentiation during AS progression by targeting *ANKH* in both AS patient-derived fibroblasts and emulsified collagen-induced AS rat models. Inhibition of miR-17-5p prevents AS progression, reduces ossification, and relieves sacroiliitis, serving as a potential therapeutic option for AS treatment.

Heterotopic ossification of ligaments is a critical histological manifestation for AS that results in pathological atypical bone formation.[20,21] The fibroblast is the primary cell type in ligaments, and osteogenic differentiation of fibroblasts accounts for osteophyte formation and ankylosis in AS.[22] We found that miR-17-5p was highly expressed in AS patient-derived ligament tissues and fibroblasts, which might lead to heterotopic ossification of ligaments. This finding was similar to the previous report that upregulation of miR-17-5p was detected in ligament-derived fibroblasts of patients with AS.[9] A number of studies suggested that miR-17-5p had a potential role in osteoblastic differentiation.[23,24] We have shown that miR-17-5p increased osteogenesis potential that was demonstrated by the detected expression patterns of osteogenesis markers (*BMP2*, *ALPL*, *RUNX2*, *COL1AL*, and *BGP*) and ALP activity in AS patient-derived fibroblasts and ligament tissues. The *in vitro* study from human-derived tissues was further confirmed in an emulsified collagen-induced AS rat model, showing that both inhibition of miR-17-5p downregulated the expression of osteogenic-related genes and ameliorated the formation of abnormal osteophytes in the ligaments around the spine in the AS rats. This observation provides the first clinical insight into the contribution of miR-17-5p to the pathophysiological regulation of heterotopic ossification of ligaments during AS progression.

Previous analysis of the molecular mechanisms revealed that miR-17-5p could regulate osteogenic differentiation by targeting several osteogenic markers, such as *BMP2*, *SMAD7*, and *SMAD5*, in different cell lines.[23,25,26] However, it was not known how miR-17-5p regulates osteogenic differentiation in AS through the regulation of *ANKH*. Both of our *in vitro* and *in vivo* strongly suggested that *ANKH* was a functional target of miR-17-5p and mediated its regulatory role in osteogenic differentiation in AS. *ANKH* has been shown to be a key regulator in the control of localized mineralization in tissues, such as bone, cartilage, and the calcified zone of the growth plate,[27] by transporting pyrophosphate from intracellular to extracellular sites, resulting in the accumulation of extracellular pyrophosphate and inhibition of mineralization. The inhibition of *ANKH* contributed to pathological mineralization and played a critical role in promoting osteogenic differentiation.[11,28] Here, we discovered that increased mineralization was accompanied by reduced *ANKH* expression in AS-derived fibroblasts. Taken together, these data suggested a possibility that decreased *ANKH* led to mineralization deposition and subsequently promoted osteogenic differentiation in AS progression. miR-17-5p regulates heterotopic ossification in AS by directly targeting and downregulating *ANKH*.

Interestingly, in our present study, in addition to findings on *ANKH*, microarray assay, PCR, and ELISA analyses revealed that miR-17-5p could inhibit DKK1 and increase VEGF expression. DKK1 is an inhibitor of the Wnt/β-catenin pathway and a vital mediator in the progression of AS.[29–31] A lower level of DKK1 leads to fusion of the sacroiliac joints by increasing WNT protein-associated osteoblast activity and new bone formation.[32,33] VEGF, a signal protein that plays a crucial role in angiogenesis, participates in endochondral ossification.[34] A higher level of VEGF is a highly specific predictor of radiographic spinal progression in patients with AS.[35] Therefore, these data implied that miR-17-5p might regulate the function of DKK1 and VEGF during AS progression, although the underlying mechanism needs further clarification.

In summary, our study elucidated a pivotal role for miR-17-5p in directing fibroblasts to osteogenic differentiation in the pathogenesis of AS. Also, we found that miR-17-5p regulated heterotopic ossification by inhibiting its direct target, *ANKH*, at the post-transcriptional level in AS. Our current observations indicate a new therapeutic option for AS through miR-17-5p inhibition.

MATERIALS AND METHODS

Human Samples

All human specimens were obtained from patients with AS (n = 20) undergoing total hip arthroplasty or non-AS patients (n = 18) undergoing surgical treatment for femoral neck fractures due to trauma at The First Affiliated Hospital of Guangxi Medical University between November 2015 and December 2017. The AS patients were diagnosed according to the modified 1984 New York criteria.[36] All patients met the diagnostic criteria. Non-AS patients were free from any immune-related disorders. Ligament tissues were obtained from the joint capsule during the surgeries. The fibroblasts were then isolated from ligament tissues and cultured in DMEM (Thermo Fisher Scientific, USA) containing 10% fetal bovine serum (FBS) (Zhejiang Tianhang Biotechnology, China), according to the method previously described.[37] The cells were collected for subsequent experiments. This study was conducted following the tenets of the Helsinki Declaration[38] and was approved by the Ethics Committee of The First Affiliated Hospital of Guangxi Medical University.

Cell Culture

Fibroblasts were isolated from the capsular ligament of patients with AS and non-AS controls. The ligament tissues were cut into 0.5 mm^3 pieces and washed twice with PBS. Ligament pieces were maintained in DMEM (Thermo Fisher Scientific, USA) containing 10% FBS (Zhejiang Tianhang Biotechnology, China) and 100 U/mL penicillin and 100 μg/mL streptomycin (Solabio, China) at 37°C in a 5% CO_2 incubator. After fibroblasts grew out of tissue fragments and adhered to the plate, the ligament pieces were removed. The culture medium was replaced once every 3 days. These cells were split at a ratio of 1:3 and cultured until the fibroblasts reached 80%–90% confluence. The fibroblasts obtained from the third passage were used for the following experiments. HEK293T cells were cultured in DMEM containing penicillin and streptomycin and supplemented with 10% FBS.

miRNA Target Prediction and Luciferase Reporter Assay

TargetScan (http://www.targetscan.org/) and microRNA.org (http://www.microrna.org/microrna/home.do) were used to predict the miR-17-5p targets. Information on the complete computational protocols is available at the corresponding websites. Then, the *ANKH* 3′ UTR sequence containing the wild-type miR-17-5p binding site (GCACTTT) and the corresponding mutant miR-17-5p binding site (TACAGGG) was amplified by PCR, subcloned into the GV272 luciferase reporter vector (Shanghai GeneChem, China), and named *ANKH*-3′ UTR-WT and *ANKH*-3′ UTR-MU, respectively. A miR-17-5p expression plasmid and its control plasmid were co-transfected with *ANKH*-3′ UTR-WT or *ANKH*-3′ UTR-MU and the respective control plasmid into HEK293T cells. Luciferase assays were performed with the dual-luciferase reporter assay system (Promega, USA), according to the manufacturer's instructions. Firefly and Renilla luciferase activity were measured consecutively 48 h after transfection by using a fluorescence microplate reader (BioTek, USA).

miR-17-5p Mimics and Inhibitor and Human Cytokine Array

For alteration of miR-17-5p expression, transient transfection of AS patient-derived fibroblasts with miR-17-5p mimics or miR-17-5p inhibitors was carried out by using Lipofectamine 2000 (Invitrogen), according to the manufacturer's procedures. All oligonucleotides were obtained from Shanghai GeneChem (Shanghai, China). Transfection efficiency was assessed by the percentage of fluorescent-positive cells, which normalized by total cell number observed under the fluorescence microscope 72 h after transfection. Human cytokine array was carried out by Threebio Technology (Shanghai, China).

Alizarin Red, H&E, and BCIP/NBT Staining

The cultured cells were stained with Alizarin red to detect calcification during heterotopic ossification. The cells in 24-well plates were washed twice with PBS and fixed for 30 min with 95% ethanol in each well. The fixed cells were stained with 1 mL of 2% Alizarin red solution (Sigma) and incubated at 37°C for 30 min. H&E and BCIP/NBT staining were performed according to the manufacturer's instructions for the respective kit used (Nanjing Jiancheng Bio-Engineering Institute, China).

Quantitative Real-Time PCR Analysis

Total RNA from cultured cells or ligament tissues was extracted using either the RNeasy Mini Kit (Qiagen, CA) or the miRNeasy Mini Kit (Qiagen, CA). The quality and concentration of RNA were detected by a spectrophotometer (NanoDrop 2000; Thermo Fisher Scientific, USA). cDNA was synthesized using the miRNA First Strand cDNA Synthesis Kit (TaKaRa, China). miRNA his-miR-17-5p and mmu-miR-17-5p were analyzed by the TaqMan MicroRNA Assay Kit (Applied Biosystems). Quantitative real-time-PCR reactions were carried out with the Power SYBR Green PCR Master Mix and a 7500 Real-Time PCR Detection System (Applied Biosystems, USA). Human and rat primers used are listed in Tables 1 and 2, respectively. The U6 small nucleolar RNA gene was used as an internal control for the normalization of miR-17-5p, and glyceraldehyde 3-phosphate dehydrogenase (*GAPDH*) was used as an internal control for the

Table 1. Primers Used in the PCR (Human)

Gene	Sense (5′–3′)	Antisense (5′–3′)
ALPL	GCAAGAAAGGGGACCCAAGA	CAGAATGTTCCACGGAGGCT
BMP2	TCCATGTGGACGCTCTTTCA	AGCAGCAACGCTAGAAGACA
Col1	GCTTCACCTACAGCGTCACT	AAGCCGAATTCCTGGTCTGG
Runx2	TGTCATGGCGGGTAACGATG	CCCTAAATCACTGAGGCGGT
BGP	TTGTGGCTCACCCTCCATCA	GGCTATTTGGGGGTCATCCG
ANKH	GAGCGCTTATAATGGAGCCG	ATCCGCAAGCTCAAGTCCAT
VEGF	ATTCCCCACTTGAATCGGGC	TCACTCACTTTGCCCCTGTC
DKK1	CTCCGGTCATCAGACTGTGC	CCGGCAAGACAGACCTTCTC
GAPDH	TCCAGTATGACTCTACCCACG	CACGACATACTCAGCACCAG
his-miR-17-5p	ACACTCCAGCTGGGCAAAGT GCTTACAGTGC	TGGTGTCGTGGAGTCG
U6	CTCGCTTCGGCAGCACA	AACGCTTCACGAATTTGCGT

Table 2. Primers Used in the PCR (Rat)

Gene	Sense (5′–3′)	Antisense (5′–3′)
ALPL	GTTACAAGGTGGTGGACGGT	ACAGTGGTCAAGGTTGGCTC
BMP2	TGCTCAGCTTCCATCACGAA	AATTTTGAGCTGGCTGTGGC
Col1	GATCCTGCCGATGTCGCTAT	GGGACTTCTTGAGGTTGCCA
Runx2	GTGGCCAGGTTCAACGATCT	TGAGGAATGCGCCCTAAA TCA
BGP	GGCGCTACCTCAACAATGGA	GGCAACACATGCCCTAAACG
ANKH	CCAACACGAACAACACGGTC	TGGGTGCCAGAACAAAGGTT
VEGF	TTGGGATCTTTCATCGGA CCA	AGAGCCCAGAAGTTGGACGA
DKK1	GGTCGTGCTTTCAACGATGG	AGGGTAGGGCTGGTAGTTGT
GAPDH	TCCAGTATGACTCTACCC ACG	CACGACATACTCAGCACCAG
rno-miR-17-5p	ACACTCCAGCTGGGCAAAG TGCTTACAGTGC	TGGTGTCGTGGAGTCG
U6	CTCGCTTCGGCAGCACA	AACGCTTCACGAATTTGCGT

normalization of target gene expression. The expression of all target genes was presented as comparative threshold cycle (ΔΔCt).

Western Blot Analysis

Total protein was isolated from cells or ligament tissues using radioimmunoprecipitation assay (RIPA) lysis buffer (Beyotime Institute of Biotechnology, Shanghai, China), according to the manufacturer's instructions. Whole cell protein extracts were qualified by bicinchoninic acid (BCA) assay (Beyotime Institute of Biotechnology, Shanghai, China). Equal amounts of protein lysates were separated with SDS-PAGE on a 12% polyacrylamide gel (Invitrogen, USA) and transferred to a nitrocellulose membrane (Bio-Rad, USA). After blocking with 5% nonfat milk in Tris-buffered saline with Tween (TBST), the membrane was washed once with TBST and incubated with antibodies against ANKH (1:200; Sigma), COL1 (1:200; Sigma), RUNX2 (1:100; Sigma), and GAPDH (1:200; Sigma) at 4°C overnight. GAPDH was used as the loading control. Signals were revealed after incubation with anti-rabbit immunoglobulin G (IgG) secondary antibody (1:5,000; Sigma) coupled to horseradish peroxidase by using enhanced chemiluminescence (ECL) (Amersham Biosciences).

Immunocytochemistry, ELISA, and ALP Activity Assay

For immunocytochemistry, fibroblasts were processed according to the manufacturer's instructions (BosterBio, China) and stained with an antibody against vimentin (1:100; Sigma). ELISA analysis for DKK1 and VEGF protein detections was carried out according to the manufacturer's instructions (Neobioscience; EHC172.96). An ELISA reader was used to detect absorption at 450 nm with matched controls. An ALP activity assay was performed according to the manufacturer's instructions (Nanjing Jiancheng Bio-Engineering Institute, China).

Animal Model

6-Week-old LEW male rats (n = 9) were selected for our research. All procedures and operations on the animals were approved by the Ethics Committee of Guangxi Medical University and were performed following accepted guidelines. For the AS rat model, the back of six rats was shaved before immunization, and each was injected intradermally with 0.1 mL of immune-stimulating reagent as one immunized site. A total of 8–10 immunized sites were induced at the back of each rat. After 2 weeks of immunization, the dosage of immune-stimulating reagent was reduced to one-half the initial dose. The immune-stimulating reagent was prepared as follows: heterologous type II collagen (CII) was dissolved in 0.1 M acetic acid at 4°C overnight. Meanwhile, bacillus Calmette-Guérin (BCG) was inactivated at 80°C and then added to 3-chloro-4-fluoroaniline (CFA) to a final concentration of 10 mg/mL. CII (1 mg/mL) and BCG (5 mg/mL) were mixed at a ratio of 1:1 and placed in an ice bath at 4°C overnight until sufficiently emulsified. After 7 days of emulsified collagen sensitization, the ankles of the rats turned red and slightly swollen. After 14 days, the rats had joint swelling, congestion, and restricted joint activity and stiffness in the spine. Skin ulcers started to appear around day 21 and accompanied with progressive deterioration of general well being, had noticeable spinal rigidity after 5 weeks. An increased arthritis index indicated a successful establishment of the AS model. After 10 weeks of immunization, one-half of these rats was injected with 3×10^8 transducing units (TU)/rat of lentivirus carrying shRNA for miR-17-5p in 100 μL PBS through tail veins. All of the animals were euthanized after 12 weeks of injection.

X-Ray and Micro-CT Analysis

Bone micro- and macro-architectures were obtained using micro-CT (SkyScan 1176; Bruker, Kontich, Belgium) and high-frequency medical diagnostic X-ray analysis (GE Definium 6000; GE Healthcare, USA).

Data Analysis

All results are presented as the mean ± SEM. Comparisons between groups were analyzed using one-way ANOVA with Turkey's post hoc test. Statistical significance was defined as $p < 0.05$.

SUPPLEMENTAL INFORMATION

Supplemental Information can be found online at https://doi.org/10.1016/j.omtn.2019.10.003.

AUTHOR CONTRIBUTIONS

X.Q., B.Z., and T.J. conducted the experiments and wrote the paper. J.T., Z.W., and Z.Y. conducted collection of samples. L.Z. and J.Z. designed the experiments and wrote the paper.

CONFLICTS OF INTEREST

The authors declare no competing interests.

ACKNOWLEDGMENTS

This study was financially supported by National Key R&D Program of China (2018YFC1105900), the Guangxi Science and Technology Base and Talent Special Project (grant no. GuikeAD17129012), and the local Science and Technology Development Project led by the central government (the three-D printing and digital medical platform (grant no. GuikeZY18164004).

REFERENCES

1. Ranganathan, V., Gracey, E., Brown, M.A., Inman, R.D., and Haroon, N. (2017). Pathogenesis of ankylosing spondylitis - recent advances and future directions. Nat. Rev. Rheumatol. *13*, 359–367.
2. O'Shea, F.D., Tsui, F.W., Chiu, B., Tsui, H.W., Yazdanpanah, M., and Inman, R.D. (2007). Retinol (vitamin A) and retinol-binding protein levels are decreased in ankylosing spondylitis: clinical and genetic analysis. J. Rheumatol. *34*, 2457–2459.
3. van der Heijde, D., Braun, J., Deodhar, A., Baraliakos, X., Landewé, R., Richards, H.B., Porter, B., and Readie, A. (2019). Modified stoke ankylosing spondylitis spinal score as an outcome measure to assess the impact of treatment on structural progression in ankylosing spondylitis. Rheumatology (Oxford) *58*, 388–400.
4. Huang, C.H., Wei, J.C., Chang, W.C., Chiou, S.Y., Chou, C.H., Lin, Y.J., Hung, P.H., and Wong, R.H. (2014). Higher expression of whole blood microRNA-21 in patients with ankylosing spondylitis associated with programmed cell death 4 mRNA expression and collagen cross-linked C-telopeptide concentration. J. Rheumatol. *41*, 1104–1111.
5. Li, Z., Wong, S.H., Shen, J., Chan, M.T., and Wu, W.K. (2016). The Role of MicroRNAs in Ankylosing Spondylitis. Medicine (Baltimore) *95*, e3325.
6. Qian, B.P., Ji, M.L., Qiu, Y., Wang, B., Yu, Y., Shi, W., and Luo, Y.F. (2016). Identification of Serum miR-146a and miR-155 as Novel Noninvasive Complementary Biomarkers for Ankylosing Spondylitis. Spine *41*, 735–742.
7. Huang, J., Song, G., Yin, Z., Luo, X., and Ye, Z. (2014). Elevated miR-29a expression is not correlated with disease activity index in PBMCs of patients with ankylosing spondylitis. Mod. Rheumatol. *24*, 331–334.
8. Chen, L., Al-Mossawi, M.H., Ridley, A., Sekine, T., Hammitzsch, A., de Wit, J., Simone, D., Shi, H., Penkava, F., Kurowska-Stolarska, M., et al. (2017). miR-10b-5p is a novel Th17 regulator present in Th17 cells from ankylosing spondylitis. Ann. Rheum. Dis. *76*, 620–625.
9. Zhang, C., Wang, C., Jia, Z., Tong, W., Liu, D., He, C., Huang, X., and Xu, W. (2017). Differentially expressed mRNAs, lncRNAs, and miRNAs with associated co-expression and ceRNA networks in ankylosing spondylitis. Oncotarget *8*, 113543–113557.
10. Hong, P., Jiang, M., and Li, H. (2014). Functional requirement of dicer1 and miR-17-5p in reactive astrocyte proliferation after spinal cord injury in the mouse. Glia *62*, 2044–2060.
11. Williams, C.J. (2016). The role of ANKH in pathologic mineralization of cartilage. Curr. Opin. Rheumatol. *28*, 145–151.
12. Huitema, L.F., and Vaandrager, A.B. (2007). What triggers cell-mediated mineralization? Front. Biosci. *12*, 2631–2645.
13. Timms, A.E., Zhang, Y., Bradbury, L., Wordsworth, B.P., and Brown, M.A. (2003). Investigation of the role of ANKH in ankylosing spondylitis. Arthritis Rheum. *48*, 2898–2902.
14. Carr, G., Moochhala, S.H., Eley, L., Vandewalle, A., Simmons, N.L., and Sayer, J.A. (2009). The pyrophosphate transporter ANKH is expressed in kidney and bone cells and colocalises to the primary cilium/basal body complex. Cell. Physiol. Biochem. *24*, 595–604.
15. Ho, A.M., Johnson, M.D., and Kingsley, D.M. (2000). Role of the mouse ank gene in control of tissue calcification and arthritis. Science *289*, 265–270.
16. Tsui, F.W., Tsui, H.W., Cheng, E.Y., Stone, M., Payne, U., Reveille, J.D., Shulman, M.J., Paterson, A.D., and Inman, R.D. (2003). Novel genetic markers in the 5′-flanking region of ANKH are associated with ankylosing spondylitis. Arthritis Rheum. *48*, 791–797.
17. Liu, Z., Cui, Y., Zhou, X., Zhang, X., and Han, J. (2013). Association of mineralization-related genes TNAP and ANKH polymorphisms with ankylosing spondylitis in the Chinese Han population. Biosci. Trends *7*, 89–92.
18. Poddubnyy, D., Rudwaleit, M., Haibel, H., Listing, J., Märker-Hermann, E., Zeidler, H., Braun, J., and Sieper, J. (2012). Effect of non-steroidal anti-inflammatory drugs on radiographic spinal progression in patients with axial spondyloarthritis: results from the German Spondyloarthritis Inception Cohort. Ann. Rheum. Dis. *71*, 1616–1622.
19. Sieper, J., and Poddubnyy, D. (2017). Axial spondyloarthritis. Lancet *390*, 73–84.
20. Crowgey, E.L., Wyffels, J.T., Osborn, P.M., Wood, T.T., and Edsberg, L.E. (2018). A Systems Biology Approach for Studying Heterotopic Ossification: Proteomic Analysis of Clinical Serum and Tissue Samples. Genomics Proteomics Bioinformatics *16*, 212–220.
21. Lee, C.K., Yoon, D.H., Kim, K.N., Yi, S., Shin, D.A., Kim, B., Lee, N., and Ha, Y. (2016). Characteristics of Cervical Spine Trauma in Patients with Ankylosing Spondylitis and Ossification of the Posterior Longitudinal Ligament. World Neurosurg. *96*, 202–208.
22. Zou, Y.C., Yang, X.W., Yuan, S.G., Zhang, P., and Li, Y.K. (2016). Celastrol inhibits prostaglandin E2-induced proliferation and osteogenic differentiation of fibroblasts isolated from ankylosing spondylitis hip tissues in vitro. Drug Des. Devel. Ther. *10*, 933–948.
23. Jia, J., Feng, X., Xu, W., Yang, S., Zhang, Q., Liu, X., Feng, Y., and Dai, Z. (2014). MiR-17-5p modulates osteoblastic differentiation and cell proliferation by targeting SMAD7 in non-traumatic osteonecrosis. Exp. Mol. Med. *46*, e107.
24. Wei, B., Wei, W., Zhao, B., Guo, X., and Liu, S. (2017). Long non-coding RNA HOTAIR inhibits miR-17-5p to regulate osteogenic differentiation and proliferation in non-traumatic osteonecrosis of femoral head. PLoS One *12*, e0169097.
25. Fang, T., Wu, Q., Zhou, L., Mu, S., and Fu, Q. (2016). miR-106b-5p and miR-17-5p suppress osteogenic differentiation by targeting Smad5 and inhibit bone formation. Exp. Cell Res. *347*, 74–82.
26. Li, H., Li, T., Wang, S., Wei, J., Fan, J., Li, J., Han, Q., Liao, L., Shao, C., and Zhao, R.C. (2013). miR-17-5p and miR-106a are involved in the balance between osteogenic and adipogenic differentiation of adipose-derived mesenchymal stem cells. Stem Cell Res. (Amst.) *10*, 313–324.
27. Gurley, K.A., Reimer, R.J., and Kingsley, D.M. (2006). Biochemical and genetic analysis of ANK in arthritis and bone disease. Am. J. Hum. Genet. *79*, 1017–1029.
28. Cao, M., Zhou, Y., Mao, J., Wei, P., Chen, D., Wang, R., Cai, Q., and Yang, X. (2019). Promoting osteogenic differentiation of BMSCs via mineralization of polylactide/gelatin composite fibers in cell culture medium. Mater. Sci. Eng. C *100*, 862–873.
29. Daoussis, D., Liossis, S.N., Solomou, E.E., Tsanaktsi, A., Bounia, K., Karampetsou, M., Yiannopoulos, G., and Andonopoulos, A.P. (2010). Evidence that Dkk-1 is dysfunctional in ankylosing spondylitis. Arthritis Rheum. *62*, 150–158.
30. Yucong, Z., Lu, L., Shengfa, L., Yongliang, Y., Ruguo, S., and Yikai, L. (2014). Serum functional dickkopf-1 levels are inversely correlated with radiographic severity of ankylosing spondylitis. Clin. Lab. *60*, 1527–1531.
31. Zou, Y.C., Yang, X.W., Yuan, S.G., Zhang, P., Ye, Y.L., and Li, Y.K. (2016). Downregulation of dickkopf-1 enhances the proliferation and osteogenic potential of fibroblasts isolated from ankylosing spondylitis patients via the Wnt/β-catenin signaling pathway in vitro. Connect. Tissue Res. *57*, 200–211.

32. Uderhardt, S., Diarra, D., Katzenbeisser, J., David, J.P., Zwerina, J., Richards, W., Kronke, G., and Schett, G. (2010). Blockade of Dickkopf (DKK)-1 induces fusion of sacroiliac joints. Ann. Rheum. Dis. *69*, 592–597.

33. Liao, H.T., Lin, Y.F., Tsai, C.Y., and Chou, T.C. (2018). Bone morphogenetic proteins and Dickkopf-1 in ankylosing spondylitis. Scand. J. Rheumatol. *47*, 56–61.

34. Patil, A.S., Sable, R.B., and Kothari, R.M. (2012). Occurrence, biochemical profile of vascular endothelial growth factor (VEGF) isoforms and their functions in endochondral ossification. J. Cell. Physiol. *227*, 1298–1308.

35. Poddubnyy, D., Conrad, K., Haibel, H., Syrbe, U., Appel, H., Braun, J., Rudwaleit, M., and Sieper, J. (2014). Elevated serum level of the vascular endothelial growth factor predicts radiographic spinal progression in patients with axial spondyloarthritis. Ann. Rheum. Dis. *73*, 2137–2143.

36. Raychaudhuri, S.P., and Deodhar, A. (2014). The classification and diagnostic criteria of ankylosing spondylitis. J. Autoimmun. *48-49*, 128–133.

37. Qin, X., Jiang, T., Liu, S., Tan, J., Wu, H., Zheng, L., and Zhao, J. (2018). Effect of metformin on ossification and inflammation of fibroblasts in ankylosing spondylitis: An in vitro study. J. Cell. Biochem. *119*, 1074–1082.

38. World Medical Association (2013). World Medical Association Declaration of Helsinki: ethical principles for medical research involving human subjects. JAMA *310*, 2191–2194.